Micromechanics of Smart Composite Plates with Periodically Embedded Actuators and Rapidly Varying Thickness

A. L. Kalamkarov, A. V. Georgiades, K. Challagulla, G. C. Saha

Micromechanics of Smart Composite Plates with Periodically Embedded Actuators and Rapidly Varying Thickness

A. L. KALAMKAROV,* A. V. GEORGIADES
K. CHALLAGULLA AND G. C. SAHA
Department of Mechanical Engineering, Dalhousie University
Halifax, Nova Scotia, B3J 2X4, Canada

ABSTRACT: Asymptotic homogenization models for smart composite plates with periodically arranged embedded actuators and rapidly varying thickness are derived. The formulated models enable the determination of both local fields and effective elastic, actuation, thermal expansion, and hygroscopic expansion coefficients from three-dimensional local unit cell problems. The actuation coefficients, for example piezoelectric or magnetostrictive, characterize the intrinsic transducer nature of active smart materials that can be used to induce strains and stresses in a coordinated fashion. The theory is illustrated by means of examples pertaining to thin smart composite plates of uniform thickness, rib- and wafer-reinforced smart composite structures, and sandwich smart composite plates with honeycomb filler.

KEY WORDS: smart composite plate, asymptotic homogenization, effective coefficients, actuation coefficients, ribs, wafers, honeycomb filler.

1. INTRODUCTION

IN RECENT YEARS, general homogenization models and their applications for periodic composite and reinforced structures were developed using asymptotic homogenization techniques. The mathematical framework of the asymptotic homogenization technique can be found in Bensoussan et al. [1] and Sanchez-Palencia [2]. This method is mathematically rigorous and

*Author to whom correspondence should be addressed. E-mail: alex.kalamkarov@dal.ca
Figures 5 and 9–13 appear in color online: http://jtc.sagepub.com

0892-7057/06/03 0251–26 $10.00/0 DOI: 10.1177/0892705706062182

it enables the prediction of both the local and overall averaged properties of the composite solid. Many problems in the framework of elasticity and thermoelasticity have been solved using these models [3–5].

The homogenized models of plates with periodic non-homogeneities in tangential coordinates have been developed in this way by Duvaut [6], Adrianov et al. [7], and others. A refined approach developed by Caillerie [8] in his heat conduction studies consists of applying a two-scale formalism directly to the three-dimensional problem of a thin non-homogeneous layer. Accordingly, Caillerie introduces two sets of 'rapid' coordinates. One of these, in the tangential directions, is associated with rapid periodic oscillations in the composite properties. The other is associated with the small thickness of the layer and takes into consideration that there is no periodicity in this transverse direction. The two small parameters thus described may or may not be of the same order of magnitude. Kohn and Vogelius [9], adopted this approach in their study of the pure bending of a thin, linearly elastic homogeneous plate. Kalamkarov [3] applied the modified asymptotic homogenization technique to three-dimensional elasticity and thermoelasticity problems pertaining to a curvilinear three-dimensional inhomogeneous layer with a rapidly varying thickness. As a result, the general homogenization models for composite and reinforced shells were derived. These models were then used to analyze a variety of composite and reinforced shells and plates of practical importance, and subsequently proceed to their design and optimization [4,5].

The interest in composite materials has led in recent years to their integration within such areas as the aerospace industry, civil engineering, transportation, and marine engineering. At the same time, significant advancements in MEMS, telecommunications and other fields, significantly facilitated the development of new and highly effective sensors and actuators. It would thus seem natural that the ever-expanding field of composite materials would seek ways to take advantage of and encompass these advancements in actuator and sensor technology. The merge of these domains gave birth to the so-called 'smart composite materials'. Smart composite materials are adaptive composite structures, which incorporate sensors and actuators. Depending on their type, smart composites can be classified as passive or actively controlled. Passive smart materials incorporate sensors that provide information on their state and integrity, while the actively controlled smart materials incorporate both sensors and actuators and they can perform self-adjustment or self-repair as conditions change.

Modeling of smart composite materials with integrated actuators and other related issues have been the focus of many researchers in recent

years. Aboudi [10] developed a microstructural model that encompasses both local and global effects, to analyze the behavior of resin-matrix and metal-matrix composites with embedded shape memory alloy (SMA) fibers. Choi and Lee [11] performed analytical and experimental studies on shape control of glass/epoxy composite beams with embedded SMA wire actuators. Song et al. [12] investigated active position control of honeycomb-type composite beams with SMA wires embedded in one of the face sheets. Kannan and Dasgupta [13] performed finite element studies of the behavior of multi-functional composites with embedded magnetostrictive devices.

Modeling of piezoelectric composites has become very important in view of the widespread applications of such materials. A survey by Rao and Sunar [14] has demonstrated the wide and important applications of piezoelectric materials in many branches of engineering. Rajapakse [15] developed closed-form plane strain and plane stress solutions for piezoelectric laminates. The use of piezoelectric actuators and sensors as elements of smart structures was investigated by Crawley and de Luis [16], Reddy [17], Ashida and Tauchert [18], Kalamkarov and Drozdov [19], Kalamkarov and Kolpakov [20], Kalamkarov and Georgiades [21,22], Tzou [23], Tzou and Bao [24], Wang and Rogers [25], and Tzou and Tiersten [26] among others.

It is apparent that the use of smart composite structures will be greatly facilitated if the effective properties and coefficients such as elastic, piezoelectric, thermal expansion etc. can be predicted at the design stage. In previous work, the authors developed comprehensive homogenization models for general three-dimensional small composite structures with homogeneous boundary conditions [21] and with more general boundary conditions where the existence of so-called boundary-layer type solutions were shown to arise [22]. The present study however, deals specifically with a smart composite plate of rapidly varying thickness and a periodic array of embedded actuators. The models derived are quite general so that the variation of the thickness of the composite structure may be attributed to either the existence of reinforcements such as ribs and stiffeners, or to the surface attachment of the actuating elements. The clear objective of the work is to construct fundamental micromechanical models that illustrate the development and use of the effective coefficients. Although some of the examples chosen for illustration purposes pertain to piezoelectric components, the analysis presented should be considered to hold equally well if the material in question is associated with some other transduction characteristics that can be used to induce strains and stresses. The model is applied to thin smart composite plates of uniform thickness, rib- and wafer-reinforced smart

composite structures, and sandwich smart composite plates with honeycomb filler.

1.1 Smart Structures with Rapidly Varying Thickness

A main objective of the work in this study involves determining the effective coefficients of smart composite structures with rapidly varying thickness. The practically important structures that are considered are (a) rib-reinforced smart composite plates, (b) smart sandwich plates with rib-like filler, (c) wafer-reinforced smart composite plates, and (d) sandwich smart composite plates with honeycomb filler. These structures are shown in Figures 1–4. The unit cells shown are the basic periodic units that repeat themselves in the x_1–x_2 plane to generate the smart structures.

2. PROBLEM FORMULATION

To analyze the smart composites shown in Figures 1–4, one must develop the equations characterizing the behavior of a generalized thin composite structure with wavy surfaces and containing a large number of periodically arranged actuators as shown in Figure 5. This periodic structure is obtained by repeating a certain small unit cell Ω_δ in the x_1–x_2 plane. All three coordinates in Figure 5 are assumed to have been made dimensionless by dividing by a certain characteristic dimension of the body, L. Note that the shape of the lateral surface of the layer is determined by the type of surface reinforcement, for example by shape of stiffeners or reinforcing ribs. The unit cell of the problem is characterized by the following inequalities (Figure 5):

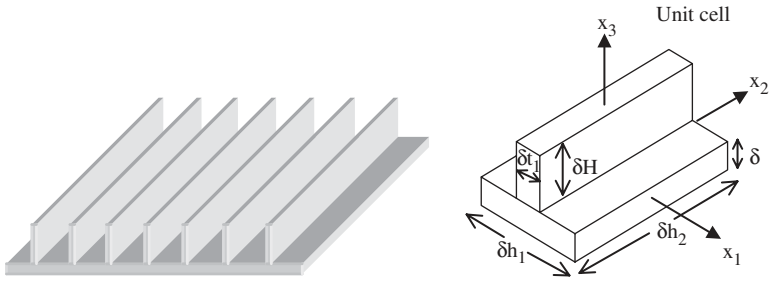

Figure 1. *A rib-reinforced smart composite plate and its unit cell.*

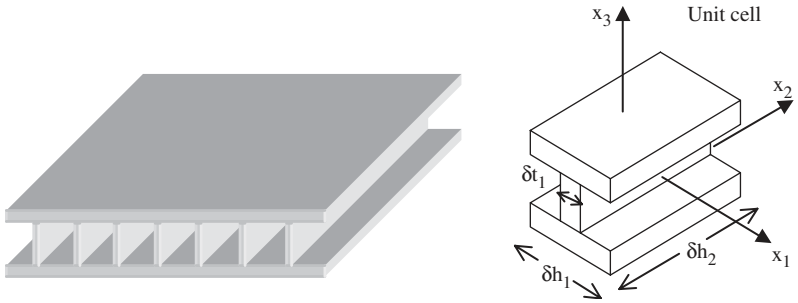

Figure 2. *A smart sandwich plate with rib-like filler and its unit cell.*

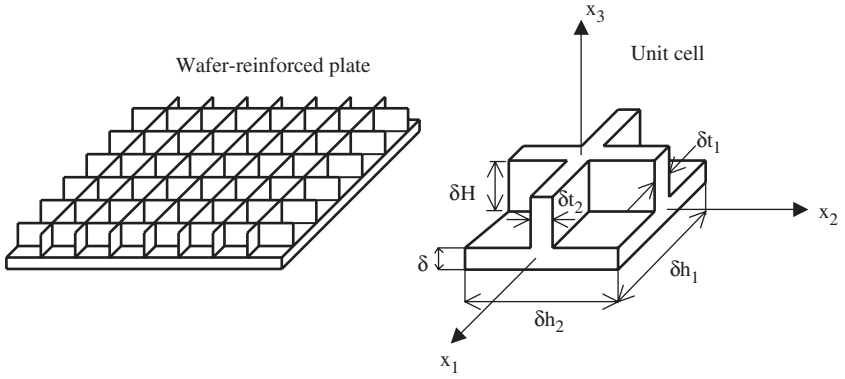

Figure 3. *A wafer-reinforced plate and its unit cell.*

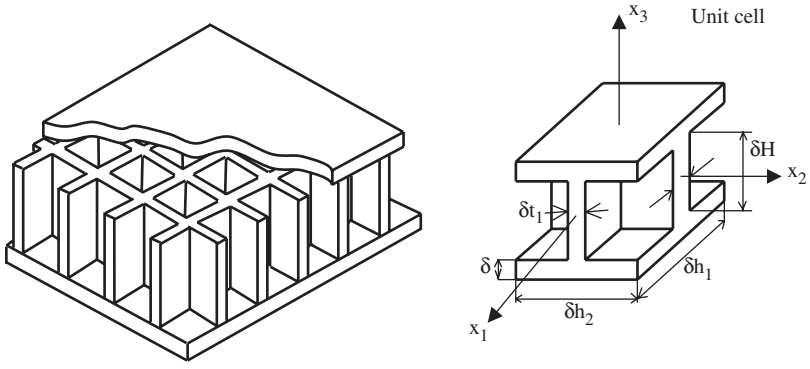

Figure 4. *A sandwich composite plate with honeycomb filler and its unit cell.*

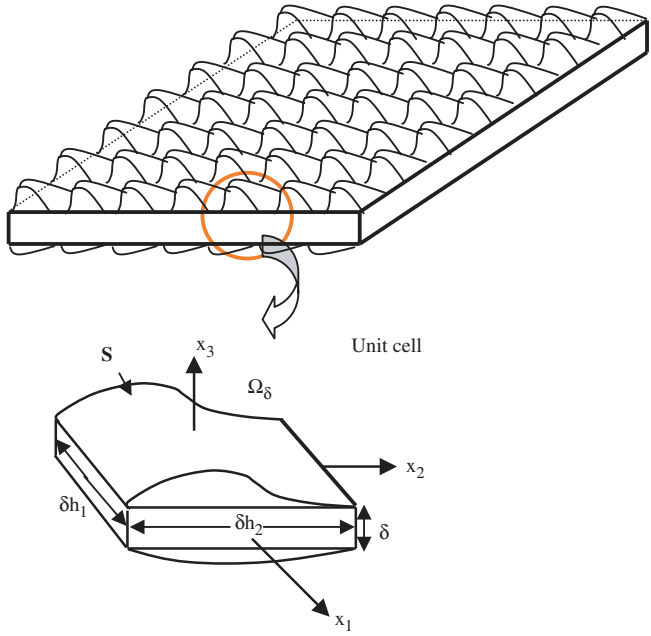

Figure 5. *Thin three-dimensional smart composite solid of a periodic structure and its unit cell.*

$$\left\{-\frac{\delta h_1}{2} < x_1 < \frac{\delta h_1}{2},\ -\frac{\delta h_2}{2} < x_2 < \frac{\delta h_2}{2},\ S^- < x_3 < S^+\right\},$$
$$\text{where} \quad S^{\pm} = \pm\frac{\delta}{2} \pm \delta F^{\pm}\left(\frac{x_1}{\delta h_1}, \frac{x_2}{\delta h_2}\right) \tag{2.1}$$

The elastic deformation of this smart structure is characterized by the following system:

$$\begin{aligned} &\sigma_{ij,jx} - P_i = 0 \quad \text{where,} \\ &\sigma_{ij} = C_{ijkl}\left\{e_{kl} - d^{(r)}_{klm}R_m - \alpha^{(\theta)}_{kl}T - \beta^{(c)}_{kl}C\right\} \text{ and} \\ &e_{ij} = \frac{1}{2}\left(u_{i,jx} + u_{j,ix}\right) \end{aligned} \tag{2.2}$$

Here, C_{ijkl} is the tensor of elastic coefficients, e_{kl} is the strain tensor which is a function of the displacement field $\mathbf{u}$, $d^{(r)}_{ijk}$ is a tensor of actuation (such as piezoelectric) coefficients describing the effect of a

control signal **R** on the stress field σ_{ij}, $\alpha_{ij}^{(\theta)}$ is the thermal expansion tensor, and $\beta_{ij}^{(c)}$ is the hygroscopic expansion tensor. Finally, T and C represent changes in the temperature and moisture content (with respect to a reference hygrothermal state) respectively. It is assumed that $C_{ijkl}, d_{ijk}^{(r)}, \alpha_{ij}^{(\theta)}, \beta_{ij}^{(c)}$ are periodic in x_1 and x_2 with respective periods δh_1 and δh_2 but are not periodic in the transverse coordinate x_3. Finally note that throughout this work, partial derivatives will be denoted as follows:

$$\psi_{ij,kx} = \frac{\partial \psi_{ij}}{\partial x_k} \quad \text{and} \quad \vartheta_{ij,ky} = \frac{\partial \vartheta_{ij}}{\partial y_k} \tag{2.3}$$

Assume that the top and bottom surfaces of the plate $S^{\pm}$ are subjected to surface tractions p_i (not to be confused with the body forces P_i) which are related to stresses by Cauchy boundary conditions,

$$\sigma_{ij} n_j = p_i \tag{2.4}$$

where for the surfaces $x_3 = S^{\pm}$ (x_1, x_2) we have the following unit normal vector:

$$\mathbf{n}^{\pm} = \frac{\left(\mp S_{1,x}^{\pm}, \mp S_{2,x}^{\pm}, 1\right)}{\sqrt{\left(S_{1,x}^{\pm}\right)^2 + \left(S_{2,x}^{\pm}\right)^2 + 1}} \tag{2.5}$$

3. ASYMPTOTIC ANALYSIS AND ASSUMPTIONS

Analysis begins with the introduction of the 'fast' variables,

$$y_1 = \frac{x_1}{\delta h_1}, \quad y_2 = \frac{x_2}{\delta h_2}, \quad z = \frac{x_3}{\delta} \tag{3.1}$$

remembering that δ is the thickness of the smart layer. The introduction of the fast variables is in recognition of the fact that the field variables have both periodic and non-periodic components and become functions of **x** and **y**. As well, the derivatives transform according to the following relationships:

$$\frac{\partial}{\partial x_\alpha} \to \frac{\partial}{\partial x_\alpha} + \frac{1}{\delta h_\alpha}\frac{\partial}{\partial y_\alpha} \quad \text{and} \quad \frac{\partial}{\partial x_3} = \frac{1}{\delta}\frac{\partial}{\partial z} \tag{3.2}$$

The use of the fast variables also means that the unitcell Ω_δ is now defined by:

$$\left\{-\frac{1}{2} < y_1 < \frac{1}{2}, \quad -\frac{1}{2} < y_2 < \frac{1}{2}, \quad Z^- < z < Z^+\right\},$$
$$\text{where } Z^\pm = \pm\frac{1}{2} \pm F^\pm(y) \tag{3.3}$$

Subsequently, the following asymptotic assumptions are made:

$$\begin{aligned} p_\alpha^\pm &= \delta^2 r_\alpha(\mathbf{x},\mathbf{y}), \quad p_3^\pm = \delta^3 q_3^\pm(\mathbf{x},\mathbf{y}) \\ P_\alpha &= \delta f_\alpha(\mathbf{x},\mathbf{y},\mathbf{z}), \quad P_3 = \delta^2 g_3(\mathbf{x},\mathbf{y},\mathbf{z}) \\ d_{ijk}^{(r)} &= \delta d_{ijk}(\mathbf{y},\mathbf{z}), \quad \alpha_{kl}^{(\theta)} = \delta\alpha_{kl}(\mathbf{y},\mathbf{z}), \quad \beta_{kl}^{(c)} = \delta\beta_{kl}(\mathbf{y},\mathbf{z}) \end{aligned} \tag{3.4}$$

$$\begin{aligned} T &= T^{(o)}(\mathbf{x}) + zT^{(1)}(\mathbf{x}) \\ C &= C^{(o)}(\mathbf{x}) + zC^{(1)}(\mathbf{x}) \\ R_i &= R_i^{(o)}(\mathbf{x}) + zR_i^{(1)}(\mathbf{x}) \end{aligned} \tag{3.5}$$

Equation (3.5) assumes linear through-the-thickness relationships for T, C, and R_i. We are justified in making this approximation on account of the small thickness of the smart structure in comparison to its in-plane dimensions. It should also be noted that in Equation (3.4) and in the sequel Greek indices will be assumed to take on the values of 1 and 2, and Latin indices will vary from 1 to 3.

The next step is to assume asymptotic expansions for the displacement and stress fields in the form of:

$$u_i = u_i^{(0)}(\mathbf{x}) + \delta u_i^{(1)}(\mathbf{x},\mathbf{y},\mathbf{z}) + \delta^2 u_i^{(2)}(\mathbf{x},\mathbf{y},\mathbf{z}) + \cdots \tag{3.6}$$

$$\sigma_{ij} = \sigma_{ij}^{(0)}(\mathbf{x},\mathbf{y},\mathbf{z}) + \delta\sigma_{ij}^{(1)}(\mathbf{x},\mathbf{y},\mathbf{z}) + \delta^2\sigma_{ij}^{(2)}(\mathbf{x},\mathbf{y},\mathbf{z}) + \cdots \tag{3.7}$$

From Equations (2.2) and (3.6), one arrives, after equating like powers of δ, at the following analogous asymptotic expansion for the strain field,

$$e_{ij} = e_{ij}^{(0)} + \delta e_{ij}^{(1)} + \delta^2 e_{ij}^{(2)} + \cdots \tag{3.8}$$

where the various terms are functions of the type $u_i^{(j)}$.

4. EQUILIBRIUM EQUATIONS AND BOUNDARY CONDITIONS

The substitution of Equation (3.7) into Equation (2.2) gives, on account of the relationships (3.2), the following system of differential equations:

$$\begin{aligned}
&\left(\frac{1}{h_\beta}\right)\sigma^{(0)}_{i\beta,\beta y} + \sigma^{(0)}_{i3,z} = 0\\
&\sigma^{(0)}_{i\beta,\beta x} + \left(\frac{1}{h_\beta}\right)\sigma^{(1)}_{i\beta,\beta y} + \sigma^{(1)}_{i3,z} = 0\\
&\sigma^{(1)}_{i\beta,\beta x} + \left(\frac{1}{h_\beta}\right)\sigma^{(2)}_{i\beta,\beta y} + \sigma^{(2)}_{i3,z} = f_i \text{ and}\\
&\sigma^{(2)}_{i\beta,\beta x} + \left(\frac{1}{h_\beta}\right)\sigma^{(3)}_{i\beta,\beta y} + \sigma^{(3)}_{i3,z} = g_i
\end{aligned} \tag{4.1}$$

The corresponding boundary conditions follow from Equations (2.4) and (3.7) and are,

$$\begin{aligned}
&\sigma^{(0)}_{ij} N^{\pm}_j = 0,\\
&\sigma^{(1)}_{ij} N^{\pm}_j = 0,\\
&\sigma^{(2)}_{ij} N^{\pm}_j = \pm\omega^{\pm} r^{\pm}_i \quad \text{and}\\
&\sigma^{(3)}_{ij} N^{\pm}_j = \pm\omega^{\pm} q^{\pm}_i,
\end{aligned} \tag{4.2}$$

where the following definitions are made:

$$\begin{aligned}
&N^{\pm} = \left(\mp\left(\frac{1}{h_1}\right)F^{\pm}_{1,y}, \mp\left(\frac{1}{h_1}\right)F^{\pm}_{2,y}, 1\right) \quad \text{and}\\
&\omega^{\pm} = \sqrt{1 + \left(\frac{1}{h_2}\right)^2\left(F^{\pm}_{1,y}\right)^2 + \left(\frac{1}{h_2}\right)^2\left(F^{\pm}_{2,y}\right)^2}.
\end{aligned} \tag{4.3}$$

5. DETERMINATION OF UNIT CELL PROBLEMS

The solution for the first terms in the asymptotic expansions of the stress and displacement fields, (Equations (3.6) and (3.7)), is the same as for the

purely elastic problem solved by Kalamkarov [3] and is given by:

$$\sigma_{ij}^{(0)} = 0 \tag{5.1}$$

$$u_1^{(0)} = u_2^{(0)} = 0, \quad u_3^{(0)} = w(\mathbf{x})$$

$$u_\nu^{(1)} = v_\nu^{(1)}(\mathbf{x}) - z w_{,\nu x}, \quad u_3^{(1)} = v_3^{(1)}(\mathbf{x}) \tag{5.2}$$

$$u_m^{(1)} = U_m^{k\alpha}(\mathbf{y}, \mathbf{z})\, \varepsilon_{k\alpha}^{(0)}(\mathbf{x}) + v_m^{(1)}(\mathbf{x}). \tag{5.3}$$

Here, $v_m^{(1)}$ is the homogeneous solution that satisfies

$$D_{ik} v_k^{(1)} = 0, \tag{5.4}$$

and $U_m^{k\alpha}$ the particular solution that satisfies

$$\begin{aligned} &D_{ik} U_k^{m\alpha} = -C_{im\alpha} \quad \text{and} \\ &\left(L_{ijk} U_k^{m\alpha} + C_{ijm\alpha}\right) N_j^{\pm} = 0 \quad \text{on } Z^{\pm}. \end{aligned} \tag{5.5}$$

In the latter expressions, the following operators are defined:

$$\begin{aligned} L_{ijk} &= C_{ijk\alpha}\left(\frac{1}{h_\alpha}\right)\frac{\partial}{\partial y_\alpha} + C_{ijk3}\frac{\partial}{\partial z}, \\ D_{ij} &= \left(\frac{1}{h_\alpha}\right)\frac{\partial}{\partial y_\alpha} L_{i\alpha j} + \frac{\partial}{\partial z} L_{i3j}, \quad \text{and} \\ C_{i\alpha j} &= \left(\frac{1}{h_\beta}\right)\frac{\partial C_{i\beta\alpha j}}{\partial y_\beta} + \frac{\partial C_{i3\alpha j}}{\partial z}. \end{aligned} \tag{5.6}$$

Also, the strain terms $\varepsilon_{k\alpha}^{(0)}(\mathbf{x})$ that appear in Equation (5.3) are defined by:

$$2\varepsilon_{ij}^{(0)} = C_{ijk\beta}\left(u_{k,\beta x}^{(0)} + u_{\beta,kx}^{(0)}\right). \tag{5.7}$$

We are now in a position to solve for the second term of the asymptotic expansion of the stress field. From Equations (3.4), (3.8), (5.3), and (2.2) we arrive at:

$$\begin{aligned} \sigma_{ij}^{(1)} = {} & L_{ijk} u_k^{(2)} + C_{ijk\beta}\varepsilon_{k\beta}^{(1)} + z C_{ij\alpha\beta}\tau_{\alpha\beta} - P_{ijk} R_k^{(0)} - Z P_{ijk} R_k^{(1)} + \\ & - K_{ij} T^{(0)} - z K_{ij} T^{(1)} - B_{ij} C^{(0)} - z B_{ij} C^{(1)} \end{aligned} \tag{5.8}$$

where,

$$2\varepsilon^{(1)}_{\alpha\beta} = \left(v^{(1)}_{\alpha,\beta x} + v^{(1)}_{\beta,\alpha x}\right), \quad \tau_{\alpha\beta} = \frac{-\partial^2 w}{\partial x_\alpha \partial x_\beta}, \quad P_{ijm} = C_{ijkl} d_{klm},$$
$$K_{ij} = C_{ijkl}\alpha_{kl}, \quad B_{ij} = C_{ijkl}\beta_{kl} \tag{5.9}$$

Furthermore, the solution for $u^{(2)}_k$ follows from Equations (4.1), (4.3), and (5.8) and is:

$$D_{ik}u^{(2)}_k = -c_{ik\alpha}\varepsilon^{(1)}_{k\alpha} - \left(C_{i3\alpha\mu} + zc_{i\alpha\mu}\right)\tau_{\alpha\mu} + P^*_{ik}R^{(0)}_k + \left(P_{i3k} + zP^*_{ik}\right)R^{(1)}_k + \\ + K^*_i T^{(0)} + \left(K_{i3} + zK^*_i\right)T^{(1)} + B^*_i C^{(0)} + \left(B_{i3} + zB^*_i\right)C^{(1)} \tag{5.10}$$

$$\begin{pmatrix} L_{ijk}u^{(2)}_k + C_{ijk\beta}\varepsilon^{(1)}_{k\beta} + zC_{ij\alpha\beta}\tau_{\alpha\beta} - P_{ijk}R^{(0)}_k - zP_{ijk}R^{(1)}_k + \\ -K_{ij}T^{(0)} - zK_{ij}T^{(1)} - B_{ij}C^{(0)} - zB_{ij}C^{(1)} \end{pmatrix} N^{\pm}_j = 0 \quad \text{on } Z^{\pm} \tag{5.11}$$

where the following definitions are made:

$$P^*_{ik} = \left(\frac{1}{h_\beta}\right)P_{i\beta k,\beta y} + P_{i3k,z}, \quad K^*_i = \left(\frac{1}{h_\beta}\right)K_{i\beta,\beta y} + K_{i3,z},$$
$$B^*_i = \left(\frac{1}{h_\beta}\right)B_{i\beta,\beta y} + B_{i3,z} \tag{5.12}$$

The separation of variables in each term on the right-hand-side of (5.10) prompts the solution for $u^{(2)}_k$ in the form of

$$u^{(2)}_m = U^{k\alpha}_m \varepsilon^{(1)}_{k\alpha} + V^{\beta\alpha}_m \tau_{\beta\alpha} + U^K_m R^{(0)}_k + V^{(k)}_m R^{(1)}_k + W_m T^{(0)} \\ + X_m T^{(1)} + Y_m C^{(0)} + A_m C^{(1)} \tag{5.13}$$

where use was also made of Equation (5.3). Substitution of solution (5.13) into Equations (5.10) and (5.11), leads, on account of the following definitions,

$$b^{m\alpha}_{ij} = L_{ijk}U^{m\alpha}_k + C_{ijm\alpha}, \quad b^{*\alpha\beta}_{ij} = L_{ijk}U^{\alpha\beta}_k + zC_{ij\alpha\beta}, \quad d^k_{ij} = P_{ijk} - L_{ijm}U^k_m,$$
$$d^{*k}_{ij} = zP_{ijk} - L_{ijm}V^k_m, \quad \Theta_{ij} = K_{ij} - L_{ijm}W, \quad \Theta^*_{ij} = zK_{ij} - L_{ijm}X_m,$$
$$\Lambda_{ij} = B_{ij} - L_{ijm}Y_m, \quad \Lambda^*_{ij} = zB_{ij} - L_{ijm}A_m \tag{5.14}$$

to a group of eight problems to be referred to in the sequel as unit cell problems. They are

$$\left(\frac{1}{h_\beta}\right) b^{\mu\alpha}_{i\beta,\,\beta y} + b^{\mu\alpha}_{i3,\,z} = 0, \quad \text{and} \quad b^{\mu\alpha}_{ij} N^{\pm}_{j} = 0 \quad \text{on} \quad Z^{\pm} \tag{5.15a}$$

$$\left(\frac{1}{h_\beta}\right) b^{*\mu\alpha}_{i\beta,\,\beta y} + b^{*\mu\alpha}_{i3,\,z} = 0, \quad \text{and} \quad b^{*\mu\alpha}_{ij} N^{\pm}_{j} = 0 \quad \text{on} \quad Z^{\pm} \tag{5.15b}$$

$$\left(\frac{1}{h_\beta}\right) d^{k}_{i\beta,\,\beta y} + d^{k}_{i3,\,z} = 0, \quad \text{and} \quad d^{k}_{ij} N^{\pm}_{j} = 0 \quad \left(\text{on } Z^{\pm}\right) \tag{5.15c}$$

$$\left(\frac{1}{h_\beta}\right) d^{*k}_{i\beta,\,\beta y} + d^{*k}_{i3,\,z} = 0, \quad \text{and} \quad d^{*k}_{ij} N^{\pm}_{j} = 0 \quad \left(\text{on } Z^{\pm}\right) \tag{5.15d}$$

$$\left(\frac{1}{h_\beta}\right) \Theta_{i\beta,\,\beta y} + \Theta_{i3,\,z} = 0, \quad \text{and} \quad \Theta_{ij} N^{\pm}_{j} = 0 \quad \left(\text{on } Z^{\pm}\right) \tag{5.15e}$$

$$\left(\frac{1}{h_\beta}\right) \Theta^{*}_{i\beta,\,\beta y} + \Theta^{*}_{i3,\,z} = 0, \quad \text{and} \quad \Theta^{*}_{ij} N^{\pm}_{j} = 0 \quad \left(\text{on } Z^{\pm}\right) \tag{5.15f}$$

$$\left(\frac{1}{h_\beta}\right) \Lambda_{i\beta,\,\beta y} + \Lambda_{i3,\,z} = 0, \quad \text{and} \quad \Lambda_{ij} N^{\pm}_{j} = 0 \quad \left(\text{on } Z^{\pm}\right) \tag{5.15g}$$

$$\left(\frac{1}{h_\beta}\right) \Lambda^{*}_{i\beta,\,\beta y} + \Lambda^{*}_{i3,\,z} = 0, \quad \text{and} \quad \Lambda^{*}_{ij} N^{\pm}_{j} = 0 \quad \left(\text{on } Z^{\pm}\right) \tag{5.15h}$$

These unit cell problems provide the functions $U^{\alpha\beta}_{k}(\mathbf{y},\mathbf{z}), \mathrm{V}^{\alpha\beta}_{k}(\mathbf{y},\mathbf{z})$, $U^{m}_{k}(\mathbf{y},\mathbf{z})$, $V^{m}_{k}(\mathbf{y},\mathbf{z})$ etc., which are 1-periodic in y_1 and y_2 and determine, in turn, the functions $b^{\alpha\beta}_{ij}, b^{*\alpha\beta}_{ij}, d^{k}_{ij}, d^{*k}_{ij}$ etc., needed to calculate the first non-vanishing term in the asymptotic expansion for the stress field, Equation (3.7), given by:

$$\begin{aligned}\sigma^{(1)}_{ij} = {} & b^{\alpha\beta}_{ij}\varepsilon^{(1)}_{\alpha\beta} + b^{*\alpha\beta}_{ij}\tau_{\alpha\beta} - d^{k}_{ij}R^{(0)}_{k} - d^{*k}_{ij}R^{(1)}_{k} + \\ & - \Theta_{ij}T^{(0)} - \Theta^{*}_{ij}T^{(1)} - \Lambda_{ij}C^{(0)} - \Lambda^{*}_{ij}C^{(1)}\end{aligned} \tag{5.16}$$

The expanded forms of the unit cell problems (5.15a) and (5.15c) as well as the stress fields (5.16) are given in Appendix A. These equations contain only commonly used material coefficients. As a final note, it should be remarked that unlike the unitcell problems of classical homogenization schemes [2,27], those set by Equations (5.15a)–(5.15h) depend on the boundary conditions at $Z^{\pm}$ rather than on periodicity in the z direction.

6. EFFECTIVE COEFFICIENTS

Applying the following averaging procedure,

$$\langle \psi \rangle = |\Omega_\delta|^{-1} \int_{\Omega_\delta} \psi \mathrm{d}y_1 \, \mathrm{d}y_2 \, \mathrm{d}z \tag{6.1}$$

to the functions $b_{ij}^{\alpha\beta}, b_{ij}^{*\alpha\beta}, d_{ij}^{k}, d_{ij}^{*k}, \Theta_{ij}, \Theta_{ij}^{*}, \Lambda_{ij}, \Lambda_{ij}^{*}$ obtained from the unit cell problems in Equations (5.15a)–(5.15h) gives the so-called effective elastic, $\langle b_{ij}^{\alpha\beta} \rangle, \langle b_{ij}^{*\alpha\beta} \rangle$; actuation, $\langle d_{ij}^{k} \rangle, \langle d_{ij}^{*k} \rangle$; thermal expansion, $\langle \Theta_{ij} \rangle, \langle \Theta_{ij}^{*} \rangle$; and hygroscopic expansion coefficients, $\langle \Lambda_{ij} \rangle, \langle \Lambda_{ij}^{*} \rangle$, pertinent to the smart composite with rapidly varying thickness.

To appreciate the meaning of the effective coefficients one may consider the simple case of a composite laminate of uniform thickness. The force and moment resultants acting on the laminate due to hygrothermal effects are given (e.g., Gibson [28]),

$$\begin{aligned}
\{N^T\} &= T^{(0)} \sum_{k=1}^{N} [\bar{Q}]_k \{\alpha^{(\theta)}\}_k (x_{3,k} - x_{3,k-1}), \\
\{M^T\} &= \frac{T^{(0)}}{2} \sum_{k=1}^{N} [\bar{Q}]_k \{\alpha^{(\theta)}\}_k \left(x_{3,k}^2 - x_{3,k-1}^2\right), \\
\{N^M\} &= C^{(0)} \sum_{k=1}^{N} [\bar{Q}]_k \{\beta^{(c)}\}_k (x_{3,k} - x_{3,k-1}), \\
\{M^M\} &= \frac{C^{(0)}}{2} \sum_{k=1}^{N} [\bar{Q}]_k \{\beta^{(c)}\}_k \left(x_{3,k}^2 - x_{3,k-1}^2\right),
\end{aligned} \tag{6.2}$$

where $[\bar{Q}]_k$ is the matrix of the plane stress-reduced elastic coefficients for the kth ply, and $x_{3,k}\ x_{3,k-1}$ denote the distance of that ply from the middle of the laminate. The superscripts T and M refer to thermal and hygroscopic effects respectively. Based on the work presented here, the corresponding forces and moments may be presented as:

$$\begin{aligned}
N_{\alpha\beta}^T &= \delta^2 \langle \Theta_{\alpha\beta} \rangle T^{(0)} + \delta^2 \left\langle \Theta_{\alpha\beta}^{*} \right\rangle T^{(1)}, \quad M_{\alpha\beta}^T = \delta^3 \langle z\Theta_{\alpha\beta} \rangle T^{(0)} + \delta^3 \left\langle z\Theta_{\alpha\beta}^{*} \right\rangle T^{(1)} \\
N_{\alpha\beta}^M &= \delta^2 \langle \Lambda_{\alpha\beta} \rangle C^{(0)} + \delta^2 \left\langle \Lambda_{\alpha\beta}^{*} \right\rangle C^{(1)}, \quad M_{\alpha\beta}^M = \delta^3 \langle z\Lambda_{\alpha\beta} \rangle C^{(0)} + \delta^3 \left\langle z\Lambda_{\alpha\beta}^{*} \right\rangle C^{(1)}
\end{aligned} \tag{6.3}$$

Similarly, one may define actuation force and moment resultants by the following equations:

$$\begin{aligned} N^R_{\alpha\beta} &= \delta^2\left\langle d^m_{\alpha\beta}\right\rangle R^{(0)}_m + \delta^2\left\langle d^{*m}_{\alpha\beta}\right\rangle R^{(1)}_m, \\ M^R_{\alpha\beta} &= \delta^3\left\langle z d^m_{\alpha\beta}\right\rangle R^{(0)}_m + \delta^3\left\langle z d^{*m}_{\alpha\beta}\right\rangle R^{(1)}_m \end{aligned} \tag{6.4}$$

It can be easily shown that if $T^{(1)}$ and $C^{(1)}$ are ignored, Equations (6.2) and (6.3) are equivalent. It can further be shown that the following relationships are also true [4].

$$\begin{aligned} &A_{\alpha\beta} = \delta\langle b^{\beta\beta}_{\alpha\alpha}\rangle, \quad A_{\alpha 6} = \delta\langle b^{12}_{\alpha\alpha}\rangle, \quad A_{66} = \delta\langle b^{12}_{12}\rangle, \\ &B_{\alpha\beta} = \delta^2\langle z b^{\beta\beta}_{\alpha\alpha}\rangle = \delta^2\langle b^{*\beta\beta}_{\alpha\alpha}\rangle, \quad B_{\alpha 6} = \delta^2\langle z b^{12}_{\alpha\alpha}\rangle = \delta^2\langle b^{*12}_{\alpha\alpha}\rangle, \\ &B_{66} = \delta^2\langle z b^{12}_{12}\rangle = \delta^2\langle b^{*12}_{12}\rangle \\ &D_{\alpha\beta} = \delta^3\langle z b^{*\beta\beta}_{\alpha\alpha}\rangle, \quad D_{\alpha 6} = \delta^3\langle z b^{*12}_{\alpha\alpha}\rangle, \quad D_{66} = \delta^3\langle z b^{*12}_{12}\rangle \end{aligned} \tag{6.5}$$

Here the coefficients A_{ij}, B_{ij}, and D_{ij} are the well-known extensional, coupling and bending coefficients pertinent to a composite laminate. Hence, the asymptotic model converges to the classical plate model for the case of a composite laminate with uniform thickness, and in view of Equations (6.3)–(6.5) the meaning of the effective coefficients is clear.

7. APPLICATIONS OF GENERAL MODEL & DISCUSSION

7.1 Uniform-thickness Laminates

We will illustrate our work by means of two sets of examples. The first set pertains to laminates of constant thickness, as shown in Figure 6. We will assume that all layers are made of homogeneous materials and are perfectly bonded with one another. As shown in the unit cell of Figure 6, each layer is completely determined by the parameters $\delta_1, \delta_2, \ldots, \delta_{\mathrm{M}}$ where M is the total number of layers. The thickness of the mth layer is therefore $\delta_m - \delta_{m-1}$ with $\delta_0 = 0$ and $\delta_{\mathrm{M}} = 1$. The real thickness of the mth layer as measured in the original (x_1, x_2, x_3) coordinate system is $\delta(\delta_m - \delta_{m-1})$, where δ is the thickness of the laminate (again with respect to the original coordinate system). Clearly, since material coefficients for this problem are independent of y_1 and y_2, all partial derivatives in Equations (5.15a)–(5.15h) become ordinary derivatives with respect to z and the unit cell problems can be solved in an elementary way.

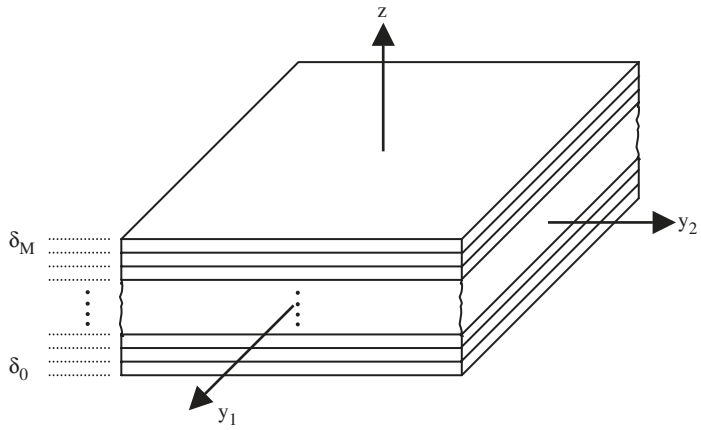

Figure 6. *Unit cell of smart composite laminate.*

Solution of the unit cell problems in Equations (5.15a)–(5.15h) and subsequent application of the averaging procedure in Equation (6.1) gives the effective coefficients. For example, the effective elastic and piezoelectric (actuation) coefficients are given by:

$$\left\langle b_{\alpha\beta}^{\lambda\mu}\right\rangle = \sum_{m=1}^{M} b_{\alpha\beta}^{\lambda\mu(m)}(\delta_m - \delta_{m-1}),$$

$$\left\langle z b_{\alpha\beta}^{\lambda\mu}\right\rangle = \left\langle b_{\alpha\beta}^{*\lambda\mu}\right\rangle = \frac{1}{2}\sum_{m=1}^{M} b_{\alpha\beta}^{\lambda\mu(m)}\left(\delta_m^2 - \delta_{m-1}^2 - (\delta_m - \delta_{m-1})\right),$$

$$\left\langle z b_{\alpha\beta}^{*\lambda\mu}\right\rangle = \left\langle z^2 b_{\alpha\beta}^{\lambda\mu}\right\rangle = \frac{1}{3}\sum_{m=1}^{M} b_{\alpha\beta}^{\lambda\mu(m)}\left(\delta_m^3 - \delta_{m-1}^3 - \frac{3}{2}\left(\delta_m^2 - \delta_{m-1}^2\right) + \frac{3}{4}(\delta_m - \delta_{m-1})\right). \tag{7.1}$$

$$\left\langle d_{\alpha\beta}^{3}\right\rangle = \sum_{m=1}^{M} d_{\alpha\beta}^{3(m)}(\delta_m - \delta_{m-1}),$$

$$\left\langle z d_{\alpha\beta}^{3}\right\rangle = \left\langle d_{\alpha\beta}^{*3}\right\rangle = \frac{1}{2}\sum_{m=1}^{M} d_{\alpha\beta}^{3(m)}\left[\left(\delta_m^2 - \delta_{m-1}^2\right) - (\delta_m - \delta_{m-1})\right],$$

$$\left\langle z d_{\alpha\beta}^{*3}\right\rangle = \left\langle z^2 d_{\alpha\beta}^{3}\right\rangle = \frac{1}{3}\sum_{m=1}^{M} d_{\alpha\beta}^{3(m)}\left[\left(\delta_m^3 - \delta_{m-1}^3\right) - \frac{3}{2}\left(\delta_m^2 - \delta_{m-1}^2\right) + \frac{3}{4}(\delta_m - \delta_{m-1})\right]. \tag{7.2}$$

Table 1. Elastic material properties [28].

Material	E_1(GPa)	E_2(GPa)	G_{12} (GPa)	ν_{12}
AS/3501 graphite/epoxy	138	9.0	6.9	0.3

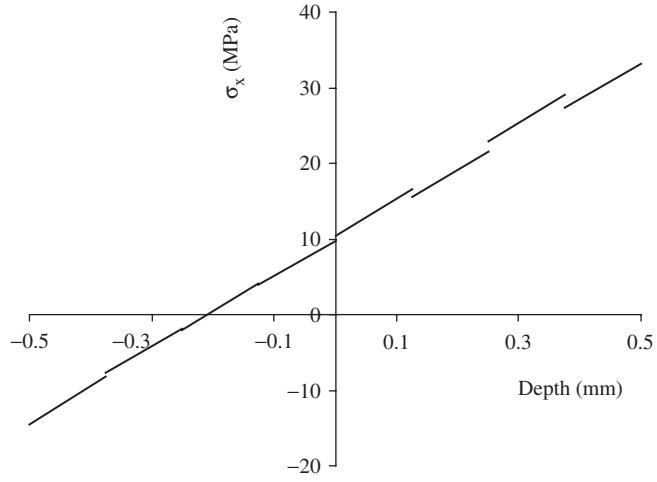

Figure 7. *Variation of σ_x through thickness of laminate.*

The use of these coefficients will be illustrated by calculating the strains and stresses in an 8-layer $[+45/-45]_4$ antisymmetric angle-ply laminate consisting of 0.125 mm thick AS/3501 graphite/epoxy laminae with material properties shown in Table 1 [28] and subjected to forces $N_x = 10\,\text{kN/m}$, $N_y = -5\,\text{kN/m}$ and moments $M_x = 4\,\text{Nm/m}$ and $M_y = -3\,\text{Nm/m}$. A typical plot is given in Figure 7 which shows the variation of σ_x. As explained above, the results are consistent with the classical plate theory to which the model converges.

The use of the effective piezoelectric coefficients will be illustrated by calculating the strains induced in a $[0/90]_4$ laminate composed of PVDF piezoelectric layers with elastic and piezoelectric properties given by Vel and Batra [29]. It will be assumed that $R_3^{(0)}$ and $R_3^{(1)}$ are both equal to 100 V/mm. A typical plot is given in Figure 8 which gives the variation of ε_x and ε_y through the thickness of the laminate. As was the case with the previous example, the results are consistent with the classical plate theory.

Similar results are obtained for the case of the effective hygroscopic and thermal expansion coefficients.

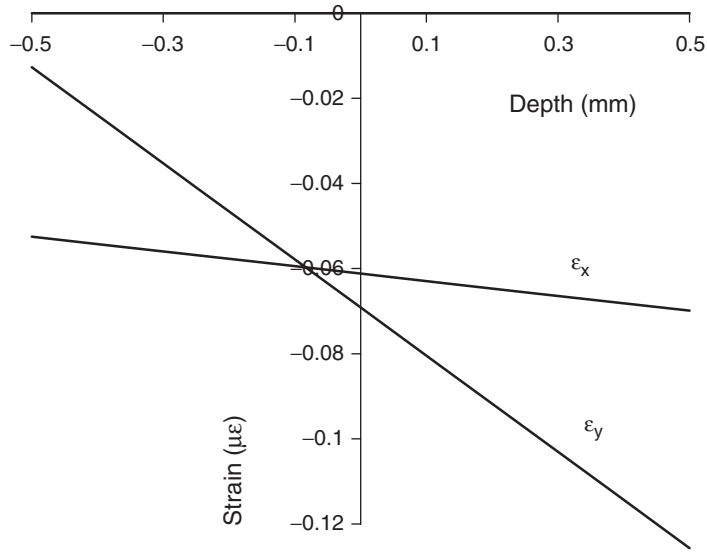

Figure 8. *Strain variation through thickness of piezoelectric laminate due to an electric field.*

7.2 Smart Composite Structures with Wafers, Ribs, and Honeycomb Fillers

The remaining examples to be considered pertain to four practically important structures. These are (a) rib-reinforced smart composite plates, (b) smart sandwich with rib-like filler, (c) wafer-reinforced smart composite plates, and (d) smart sandwich composite plates with honeycomb filler. The geometry of these structures is illustrated in Figures 1–4. For convenience, these structures will be referred to in the sequel as structures 1, 2, 3, and 4 respectively.

A solution for these types of geometry can be obtained by assuming that the thickness of each element of the unit cell (i.e., base plate, ribs etc.) is small in comparison with the other two dimensions. For example, referring to the wafer structure in Figure 3, this assumption amounts to the following:

$$t_1 << h_2, \quad t_2 << h_1, \quad H \sim h_1, h_2 \tag{7.3}$$

The local problems can then be approximately solved for each of the unit cell elements assuming that complications at the joints are highly localized and do not contribute significantly to the integrals over the unit cell.

The structures in Figures 1–4 are assumed to be made of orthotropic materials that may also exhibit piezoelectric characteristics. For generality,

each member of the unit cell may be made of a different orthotropic material. For example, for the rib-reinforced plate in Figure 1, the ribs may be piezoelectric, whereas the plate itself may not exhibit any actuation characteristics.

The determination of the effective coefficients for all three types of smart composites is obtained by solving the pertinent unit cell problems in Equations (5.15a)–(5.15h), and subsequent application of Equation (6.1). The solution steps are straightforward but rather lengthy and will not be repeated here. Instead, some representative results are given below:

$$\delta\langle\Theta_{11}\rangle = \frac{E_1^{(3)}\alpha_1^{(\theta)(3)} + E_1^{(3)}\nu_{21}^{(3)}\alpha_2^{(\theta)(3)}}{1-\nu_{12}^{(3)}\nu_{21}^{(3)}}, \quad \delta\langle z\Theta_{11}\rangle = \delta\left\langle\Theta_{11}^{*}\right\rangle = 0$$

$$\delta\langle\Theta_{22}\rangle = E_2^{(1)}\alpha_2^{(\theta)(1)}F_1^{(w)} + \frac{E_2^{(3)}\alpha_2^{(\theta)(3)} + E_2^{(3)}\nu_{12}^{(3)}\alpha_1^{(\theta)(3)}}{1-\nu_{12}^{(3)}\nu_{21}^{(3)}}, \quad \delta\langle z\Theta_{22}\rangle = E_2^{(1)}\alpha_2^{(\theta)(1)}S_1^{(w)}$$

$$\delta\left\langle z\Theta_{11}^{*}\right\rangle = \frac{E_1^{(3)}\alpha_1^{(\theta)(3)} + E_1^{(3)}\nu_{21}^{(3)}\alpha_2^{(\theta)(3)}}{12\left(1-\nu_{12}^{(3)}\nu_{21}^{(3)}\right)}$$

$$\delta\left\langle z\Theta_{22}^{*}\right\rangle = E_2^{(1)}\alpha_2^{(\theta)(1)}J_1^{(w)} + \frac{E_2^{(3)}\alpha_2^{(\theta)(3)} + E_2^{(3)}\nu_{12}^{(3)}\alpha_1^{(\theta)(3)}}{12\left(1-\nu_{12}^{(3)}\nu_{21}^{(3)}\right)} \tag{7.4}$$

Equation (7.4) gives the effective thermal expansion coefficients of structure 1. Here the superscripts (1) and (3) refer to the reinforcing element (rib) and base plate respectively, while the quantities $F_1^{(w)}, S_1^{(w)}, J_1^{(w)}$ are, respectively, the cross-sectional area, the first moment of area, and the moment of inertia of the cross-section of the rib relative to the middle surface of the base plate. The other terms in Equation (7.4) refer to the familiar material properties. Equation (7.5) gives the effective piezoelectric coefficients for structure 3. As anticipated, superscripts (1) and (2) refer to the reinforcing elements in the x_2 and x_1 directions respectively, and superscript (3) refers to the base plate. Similar results are obtained for all the other effective coefficients pertinent to all of structures 1–4:

$$\delta\left\langle d_{11}^{3}\right\rangle = E_1^{(2)}d_{31}^{(r)(2)}F_2^{(w)} + \frac{E_1^{(3)}d_{31}^{(r)(3)} + E_1^{(3)}\nu_{21}^{(3)}d_{32}^{(r)(3)}}{1-\nu_{12}^{(3)}\nu_{21}^{(3)}}$$

$$\delta\left\langle d_{22}^{3}\right\rangle = E_2^{(1)}d_{32}^{(r)(1)}F_1^{(w)} + \frac{E_2^{(3)}d_{32}^{(r)(3)} + E_2^{(3)}\nu_{12}^{(3)}d_{31}^{(r)(3)}}{1-\nu_{12}^{(3)}\nu_{21}^{(3)}}$$

$$\delta\langle zd_{11}^{3}\rangle = \delta\langle d_{11}^{*3}\rangle = E_1^{(2)} d_{31}^{(r)(2)} S_2^{(w)}$$

$$\delta\langle zd_{22}^{3}\rangle = \delta\langle d_{22}^{*3}\rangle = E_2^{(1)} d_{32}^{(r)(1)} S_1^{(w)}$$

$$\delta\langle zd_{11}^{*3}\rangle = E_1^{(2)} d_{31}^{(r)(2)} J_2^{(w)} + \frac{E_1^{(3)} d_{31}^{(r)(3)} + E_1^{(3)} \nu_{21}^{(3)} d_{32}^{(r)(3)}}{12\left(1 - \nu_{12}^{(3)} \nu_{21}^{(3)}\right)}$$

$$\delta\langle zd_{22}^{*3}\rangle = E_2^{(1)} d_{32}^{(r)(1)} J_1^{(w)} + \frac{E_2^{(3)} d_{32}^{(r)(3)} + E_2^{(3)} \nu_{12}^{(3)} d_{31}^{(r)(3)}}{12\left(1 - \nu_{12}^{(3)} \nu_{21}^{(3)}\right)} \tag{7.5}$$

It is of interest to plot and compare the effective coefficients for structures 1–4. Some representative plots are shown in Figures 9–13. Figure 9 compares some effective elastic coefficients of structures 1 and 3. In each case, the base plate is made of glass/epoxy material and the piezoelectric ribs and wafers are made of PZT4. The properties for these

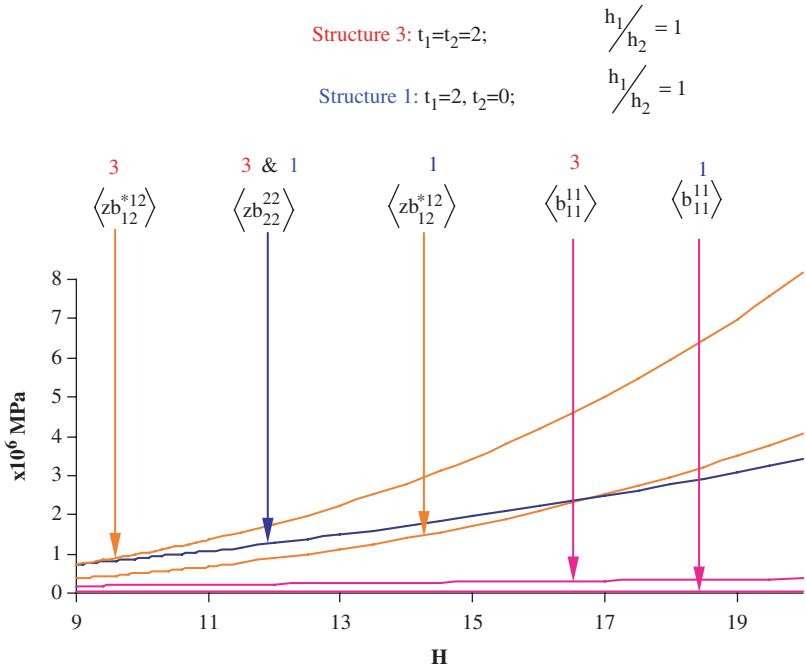

Figure 9. *Plot of effective elastic coefficients vs H for structures 1 and 3.*

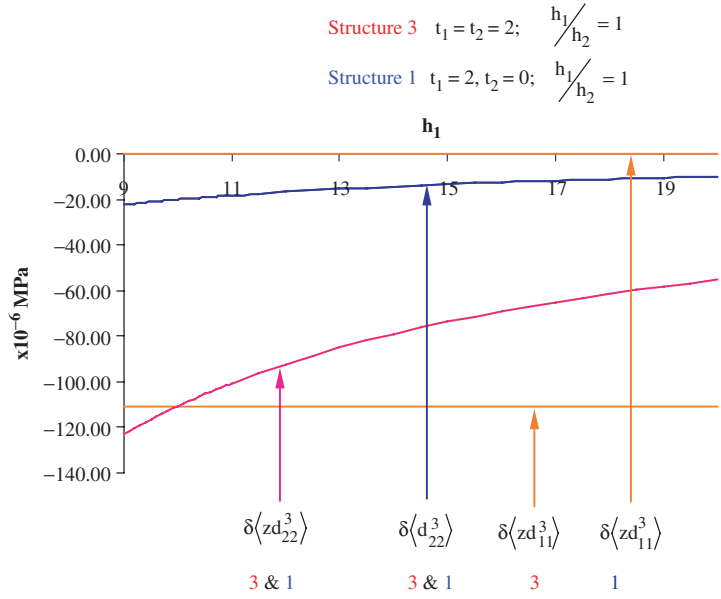

Figure 10. *Plot of effective piezoelectric coefficients vs h_1 for structures 1 and 3.*

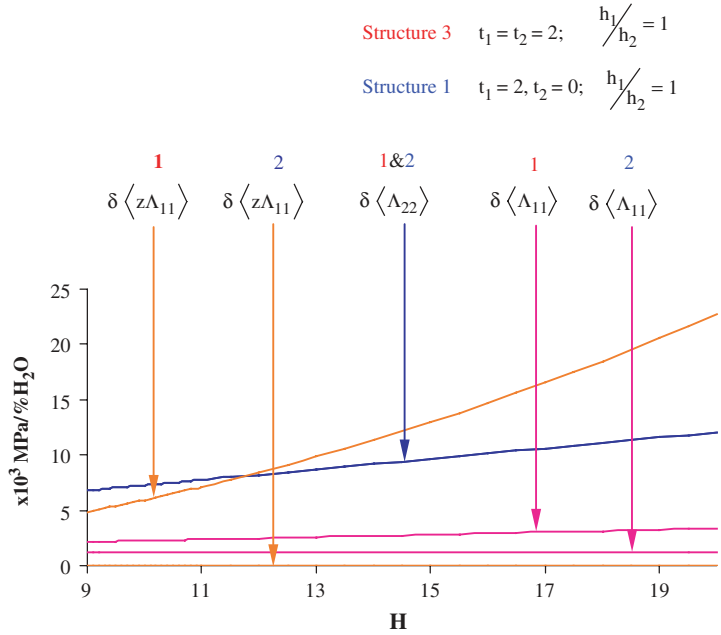

Figure 11. *Plot of effective hygroscopic expansion coefficients vs H for structures 1 and 3.*

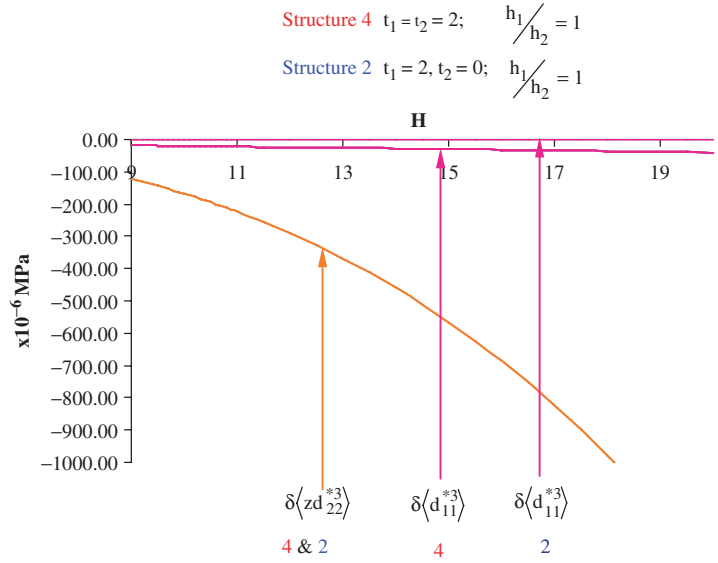

Figure 12. *Plot of effective piezoelectric coefficients vs H for structures 2 and 4.*

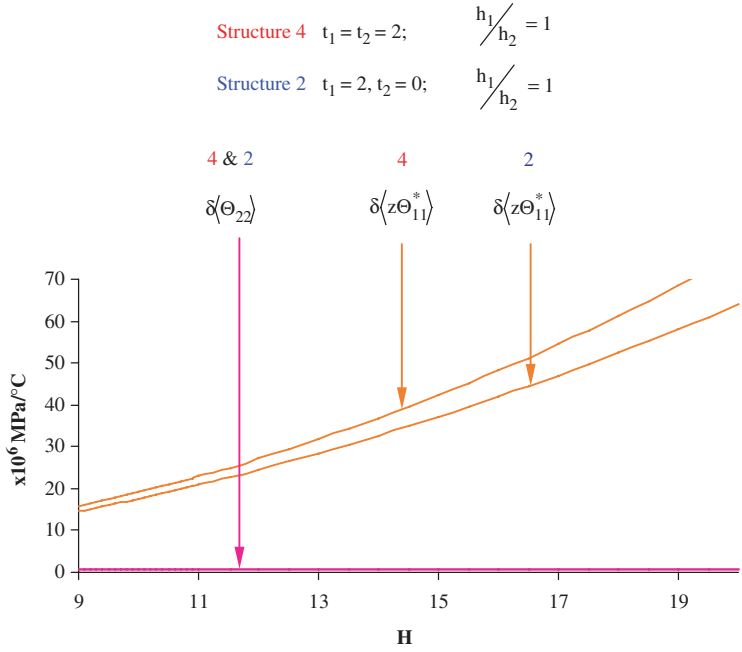

Figure 13. *Plot of effective thermal expansion coefficients vs H for structures 2 and 4.*

Table 2. Material coefficients for smart reinforced structures [28,29].

Properties	E-glass/epoxy	PZT4	PZT-5A
$E_1(10^9 Pa)$	38.6	81.23	61.0
$E_2(10^9 Pa)$	8.27	81.23	61.0
$G_{12}(10^9 Pa)$	4.14	30.6	22.6
$G_{23}(10^9 Pa)$	3.281	25.6	21.1
$G_{13}(10^9 Pa)$	4.14	25.6	21.1
ν_{12}	0.26	0.327	0.35
ν_{21}	0.055	0.327	0.35
$d_{31}(10^{-10} C/N)$	0	−1.238	−1.238
$d_{32}(10^{-10} C/N)$	0	−1.238	−1.238
β_1	0.014		
β_2	0.29		
$\alpha_1(10^{-6}/^\circ C)$	6.3		1.5
$\alpha_2(10^{-6}/^\circ C)$	20		1.5

materials can be found in Table 2 [28,29]. The plot shows the variation of the effective elastic coefficients as a function of H. As anticipated, the effective elastic coefficients are generally larger for structure 3 than for structure 1, except for $\langle z b_{22}^{22} \rangle$ (and also $\langle b_{22}^{22} \rangle$) which has the same value for both structures. This is to be expected, because these coefficients depend only on the reinforcing elements in the x_2 direction which are identical for structures 1 and 3. Figure 10 compares the effective piezoelectric coefficients of structures 1 and 3. Again, the effective piezoelectric coefficients are generally larger for structure 2 except for $\langle z d_{22}^{3} \rangle$ and $\langle d_{22}^{3} \rangle$ which are equal for both structures as expected from the geometry of the unit cells. Similar considerations apply to the effective hygroscopic expansion coefficients of Figure 11. Pertaining to this figure, both structures 1 and 3 are made entirely of E-glass/epoxy. Figure 12 compares some effective piezoelectric coefficients for structures 2 and 4. For both structures, the top and bottom carrier layers are made of E-glass/epoxy, while the middle stiffeners are made of PZT-5A piezoelectric material. As expected, the effective coefficients are generally higher for structure 4 than for structure 2, except for coefficients such as $\langle d_{22}^{3} \rangle$ and $\langle z d_{22}^{3} \rangle$ which must have the same value for both structures due to the makeup of the unit cell. Finally, Figure 13 compares some effective thermal expansion coefficients for structures 2 and 4. In this case, the entire structures are made of E-glass/epoxy. Once again, these coefficients are higher for structure 4, with the exception of $\langle \Theta_{22} \rangle$ and $\langle z \Theta_{22} \rangle$ which are identical for both structures. In summary, it is noteworthy to mention that the effective coefficients are universal in nature for a particular unit cell geometry, and they can be used to analyze a wide variety of boundary value problems.

8. CONCLUSIONS

The method of asymptotic homogenization was used to analyze a periodic smart composite plate with a large number of embedded actuators and rapidly varying thickness. A set of 8 three-dimensional local unit cell problems was derived which, unlike classical homogenization schemes, was shown to depend on boundary conditions rather than periodicity in the transverse direction. The solution of the unit cell problems allows the determination of effective elastic, actuation, thermal expansion, and hygroscopic expansion coefficients pertinent to the homogenized anisotropic smart plate. The effective coefficients in turn lead to the determination of the displacement and stress fields. In the limiting case of a thin elastic plate of uniform thickness the derived model converges to the familiar classical laminate model.

To illustrate the use of the unit cells and the applicability of the effective coefficients, two broad classes of examples were considered. The first pertained to various laminates composed of orthotropic materials. In particular, angle-ply laminates were subjected to mechanical loads and electric fields, and the effective coefficients were used to calculate the strain and stress distribution through the thickness of the laminates. It was shown that the results conformed to the classical laminate theory. The remaining examples dealt with some practically important structures, namely rib-reinforced smart composite plates, smart sandwich plates with rib-like filler, wafer-reinforced smart composite plates, and sandwich smart composite plates with honeycomb filler. The effective coefficients of these structures were determined and compared. The differences in the values of the effective coefficients were attributed to the geometries of the respective unit cells. The importance of the effective coefficients lies in the fact that they are universal in nature, and once determined they can be used to study a wide variety of boundary value problems.

ACKNOWLEDGMENT

This work has been supported by the Natural Sciences and Engineering Research Council of Canada.

APPENDIX A

The unit cell problems are given in Equations (5.15a)–(5.15h). Next, we give two of these differential equations and pertinent boundary conditions in expanded form which contain only commonly used material coefficients and the 1-periodic (in y_1 and y_2) functions $U_m^{k\alpha}$, and , U_m^k to be determined from these problems. These functions enter Equations (3.6), (5.3), and (5.13).

Thus, Equation (5.15a) becomes:

$$\frac{1}{h_\beta}\frac{\partial}{\partial y_\beta}\left\{C_{i\beta k\gamma}\frac{1}{h_\gamma}\frac{\partial U_k^{\mu\alpha}}{\partial y_\gamma}+C_{i\beta k3}\frac{\partial U_k^{\mu\alpha}}{\partial z}+C_{i\beta\mu\alpha}\right\}+$$
$$\frac{\partial}{\partial z}\left\{C_{i3k\gamma}\frac{1}{h_\gamma}\frac{\partial U_k^{\mu\alpha}}{\partial y_\gamma}+C_{i3k3}\frac{\partial U_k^{\mu\alpha}}{\partial z}+C_{i3\mu\alpha}\right\}=0 \tag{A.1}$$

$$\left\{C_{ijk\gamma}\frac{1}{h_\gamma}\frac{\partial U_k^{\mu\alpha}}{\partial y_\gamma}+C_{ijk3}\frac{\partial U_k^{\mu\alpha}}{\partial z}+C_{ij\mu\alpha}\right\}N_j^{\pm}=0 \quad \text{on} \quad Z^{\pm} \tag{A.2}$$

Likewise, Equation (5.15c) becomes:

$$\frac{1}{h_\beta}\frac{\partial}{\partial y_\beta}\left\{P_{i\beta k}-C_{i\beta m\gamma}\frac{1}{h_\gamma}\frac{\partial U_m^k}{\partial y_\gamma}-C_{i\beta m3}\frac{\partial U_m^k}{\partial z}\right\}+$$
$$\frac{\partial}{\partial z}\left\{P_{i3k}-C_{i3m\gamma}\frac{1}{h_\gamma}\frac{\partial U_m^k}{\partial y_\gamma}-C_{i3m3}\frac{\partial U_m^k}{\partial z}\right\}=0 \tag{A.3}$$

$$\left\{P_{ijk}-C_{ijm\alpha}\frac{1}{h_\alpha}\frac{\partial U_m^k}{\partial y_\alpha}-C_{ijm3}\frac{\partial U_m^k}{\partial z}\right\}N_j^{\pm}=0 \quad \text{on} \quad Z^{\pm} \tag{A.4}$$

The remaining of the unit cell problems can be written in a similar fashion. Finally, the stress field in Equation (5.16) may be written in expanded form as follows:

$$\sigma_{ij}^{(1)}=\left\{C_{ijk\gamma}\frac{1}{h_\gamma}\frac{\partial U_k^{\alpha\beta}}{\partial y_\gamma}+C_{ijk3}\frac{\partial U_k^{\alpha\beta}}{\partial z}+C_{ij\alpha\beta}\right\}\varepsilon_{\alpha\beta}^{(1)}$$
$$+\left\{C_{ijk\gamma}\frac{1}{h_\gamma}\frac{\partial V_k^{\alpha\beta}}{\partial y_\gamma}+C_{ijk3}\frac{\partial V_k^{\alpha\beta}}{\partial z}+zC_{ij\alpha\beta}\right\}\tau_{\alpha\beta}+$$
$$-\left\{P_{ijk}+C_{ijm\alpha}\frac{1}{h_\alpha}\frac{\partial U_m^k}{\partial y_\alpha}+C_{ijm3}\frac{\partial U_m^k}{\partial z}\right\}R_k^{(0)}$$
$$-\left\{zP_{ijk}+C_{ijm\alpha}\frac{1}{h_\alpha}\frac{\partial V_m^k}{\partial y_\alpha}+C_{ijm3}\frac{\partial V_m^k}{\partial z}\right\}R_k^{(1)}+$$
$$-\left\{K_{ij}+C_{ijm\alpha}\frac{1}{h_\alpha}\frac{\partial W_m}{\partial y_\alpha}+C_{ijm3}\frac{\partial W_m}{\partial z}\right\}T^{(0)}$$
$$-\left\{zK_{ij}+C_{ijm\alpha}\frac{1}{h_\alpha}\frac{\partial X_m}{\partial y_\alpha}+C_{ijm3}\frac{\partial X_m}{\partial z}\right\}T^{(1)}+$$

$$- \left\{ B_{ij} + C_{ijm\alpha} \frac{1}{h_\alpha} \frac{\partial Y_m}{\partial y_\alpha} + C_{ijm3} \frac{\partial Y_m}{\partial z} \right\} C^{(0)}$$

$$- \left\{ zB_{ij} + C_{ijm\alpha} \frac{1}{h_\alpha} \frac{\partial A_m}{\partial y_\alpha} + C_{ijm3} \frac{\partial A_m}{\partial z} \right\} C^{(1)} \tag{A.5}$$

REFERENCES

1. Bensoussan, A., Lions, J.L. and Papanicolaou, G. (1978). *Asymptotic Analysis for Periodic Structures*, North-Holland Publ. Comp., Amsterdam.
2. Sanchez-Palencia, E. (1980). *Non-Homogeneous Media and Vibration Theory*, Springer-Verlag, Berlin.
3. Kalamkarov, A.L. (1992). *Composite and Reinforced Elements of Construction*, Wiley, New York.
4. Kalamkarov, A.L. and Kolpakov, A.G. (1997). *Analysis, Design and Optimization of Composite Structures*, Wiley, New York.
5. Kalamkarov, A.L. and Kolpakov, A.G. (1996). On the Analysis and Design of Fiber Reinforced Composite Shells, *Transactions of the ASME Journal of Applied Mechanics*, **63**(4): 939–945.
6. Duvaut, G. (1976). Analyse fonctionnelle et méchanique des milieux continues, In: *Proceeding of the 14th IUTAM Congress*, pp. 119–132. Delft.
7. Andrianov, I.V., Lesnichaya, V.A. and Manevich, L.I. (1985). *Homogenization Methods in the Statics and Dynamics of Ribbed Shells*, Nauka, Moscow.
8. Caillerie, D. (1981). Homogénéisation des equation de la diffusion stationnaire dans les domaines cylindrique aplatis, *Anal. Numér.*, **15**: 295–319.
9. Kohn, R.V. and Vogelius, M. (1984). A New Model for Thin Plates with Rapidly Varying Thickness, *Int. J. of Solids and Struct.*, **20**(4): 333–350.
10. Aboudi, J. (1997). The Response of Shape Memory Alloy Composites, *Smart Mater. Struct.*, **6**(1): 1–9.
11. Choi, S. and Lee, J.J. (1998). The Shape Control of a Composite Beam with Embedded Shape Memory Alloy Wire Actuators, *Smart Mater. Struct.*, **7**(6): 759–770.
12. Song, G., Kelly, B. and Agrawal, B.N. (2000). Active Position Control of a Shape Memory Alloy Wire Actuated Composite Beam, *Smart Mater. Struct.*, **9**(5): 711–716.
13. Kannan, K.S. and Dasgupta, A. (1994). Finite Element Modeling of Multi-functional Composites with Embedded Magnetostrictive Devices, *Adaptive Structures and Composite Materials: Analysis and Application*, **45**: 21–28.
14. Rao, S.S. and Sunar, M. (1994). Piezoelectricity and its use in Disturbance Sensing and Control of Flexible Structures: A Survey, *ASME Appl. Mech. Rev.*, **47**(4): 113–123.
15. Rajapakse, R.K.N.D. (1997). Plane Strain/Stress Solutions for Piezoelectric Solids, *Composites Part B: Engineering*, **28B**(4): 385–396.
16. Crawley, E.F. and de Luis, J. (1987). Use of Piezoelectric Actuators as Elements of Intelligent Structures, *AIAA J.*, **25**(10): 1373–1385.
17. Reddy, J.N. (1999). On Laminated Composite Plates with Integrated Sensors and Actuators, *Engng. Struct.*, **21**: 568–593.
18. Ashida, F. and Tauchert, T.R. (1998). An Inverse Problem for Determination of Transient Surface Temperature from Piezoelectric Sensor Measurement, *Trans. ASME, J. Appl. Mech.*, **65**(2): 367–373.

19. Kalamkarov, A.L. and Drozdov, A.D. (1997). Optimal Design of Intelligent Composite Structures, *Journal of Intelligent Material Systems and Structures*, **8**(9): 757–766.
20. Kalamkarov, A.L. and Kolpakov, A.G. (2001). A New Asymptotic Model for a Composite Piezoelastic Plate, *Int. J. of Solids and Struct.*, **38**(34/35): 6027–6044.
21. Kalamkarov, A.L. and Georgiades, A.V. (2002). Modeling of Smart Composites on Account of Actuation, Thermal Conductivity and Hygroscopic Absorption, *Composites Part B: Engineering*, **33**(2): 141–152.
22. Kalamkarov, A.L. and Georgiades, A.V. (2002). Micromechanical Modeling of Smart Composite Structures, *Smart Mater. Struct.*, **11**(3): 423–434.
23. Tzou, H.S. (1993). *Piezoelectric Shells: Distributed Sensing and Control of Continua*, Kluwer, Dordrecht.
24. Tzou, H.S. and Bao, Y. (1995). A Theory on Anisotropic Piezothermoelastic Shell Laminates with Sensor/Actuator Applications, *J. Sound Vibra.*, **184**(3): 453–473.
25. Wang, B.T. and Rogers, C.A. (1991). Laminated Theory for Spatially Distributed Induced Strain Actuators, *J. Compos. Mater.*, **25**: 433–453.
26. Tzou, Y.S. and Tiersten, H.F. (1994). Elastic Analysis of Laminated Composite Plates in Cylindrical Bending due to Piezoelectric Actuators, *Smart Mater. Struct.*, **3**(3): 255–265.
27. Bakhvalov, N. and Panasenko, G. (1984). *Homogenisation: Averaging Processes in Periodic Media*, Kluwer Academic Publishers, Netherlands.
28. Gibson, R.F. (1994). *Principles of Composite Material Mechanics*, McGraw-Hill, New York.
29. Vel, S.S. and Batra, R.C. (2000). Three-Dimensional Analytical Solution for Hybrid Multilayered Piezoelectric Plates, *Transactions of the ASME*, **67**(3): 558–567.